# The Airborne Multi-angle Imaging SpectroRadiometer (AirMISR): Instrument Description and First Results

David J. Diner, Lisa M. Barge, Carol J. Bruegge, Thomas G. Chrien, James E. Conel, Michael L. Eastwood, Jose D. Garcia, Marco A. Hernandez, Charles G. Kurzweil, William C. Ledeboer, Neil D. Pignatano, Charles M. Sarture, and Bruce G. Smith

***Abstract*—An Airborne Multi-angle Imaging SpectroRadiometer (AirMISR) instrument has been developed to assist in validation of the Earth Observing System (EOS) MISR experiment. Unlike the EOS MISR, which contains nine individual cameras pointed at discrete look angles, AirMISR utilizes a single camera in a pivoting gimbal mount. The AirMISR camera has been fabricated from MISR brassboard and engineering model components and, thus, has similar radiometric and spectral response as the MISR cameras. This paper provides a description of the AirMISR instrument and summarizes the results of engineering flights conducted during 1997.**

***Index Terms*—Earth, remote sensing.**

## I. Introduction

THE MULTI-angle Imaging SpectroRadiometer (MISR) instrument [1], [2] is scheduled for launch in late 1998 aboard the first Earth Observing System morning spacecraft (EOS-AM1). MISR uses nine separate charge coupled device (CCD)-based pushbroom cameras to observe the earth at nine discrete angles: one at nadir plus eight other symmetrically placed cameras that provide fore–aft observations with view angles, at the earth's surface, of 26.1, 45.6, 60.0, and 70.5°, relative to the local vertical. Each camera contains four detector line arrays, each overlain by a spectral filter providing imagery at 446, 558, 672, and 866 nm, with bandwidths of 42, 29, 22, and 40 nm, respectively [3]. Samples will be acquired from the 705-km sun-synchronous near-polar orbit, with spacings ranging from 275 m–1.1 km. MISR will enable study of the effects of different types of cloud fields and tropospheric aerosol hazes on the solar radiance and irradiance reflected to space. Surface observations will enable improved measures of land surface classification and radiative characteristics.

In 1996, the EOS Project Science Office at the NASA Goddard Space Flight Center (GSFC), Greenbelt, MD, approved the construction of an airborne MISR simulator, designated AirMISR. The primary mission of AirMISR includes the following:

1) collect MISR-like data sets to support the validation of MISR geophysical retrieval algorithms and data products;
2) underfly the EOS-AM1 MISR sensor to provide an additional radiometric calibration path and to assist with in-flight instrument performance characterization; and
3) enable scientific research utilizing high-quality, well-calibrated multiangle imaging data.

A secondary mission is to serve as a technology testbed for advanced, lightweighted MISR cameras for future remote-sensing platforms.

## II. AirMISR Requirements

The most important requirement for AirMISR is that its data characteristics, to the extent possible, match the space-borne sensor it is designed to support. Thus, the performance requirements are nearly the same as those of MISR, with the primary exceptions (due to practical limitations of flying at a significantly lower altitude) being ground instantaneous field-of-view, swath width, and spatial coverage. A principal requirement is that the simulator must image the same area on the ground from all nine MISR look angles.

Prior to the advent of AirMISR, the GSFC Advanced Solid-State Array Spectroradiometer (ASAS) [4], which has flown on the NASA C-130 and P3B aircraft, has been used to develop and test some of the MISR geophysical algorithms [5]. ASAS is a 62-channel imaging spectrometer, operating in the 400–1000-nm spectral range, with 10-nm bandwidth per channel. From the C-130, the view angle range 70° forward to 55° aft is accessible; the aft range is extendable to 70° by flying in the P3B. However, in its current implementation, the swath width is 1.5–2 km, which is insufficient areal extent to test certain MISR algorithms. Other radiometric and spectral performance issues make it desirable to fly an airborne simulator with characteristics more similar to the MISR specifications. Nevertheless, ASAS has played an important role in multiangle imaging studies and can be expected to continue to do so.

The NASA ER-2 is the preferred platform for AirMISR because its flight altitude of 65 000 feet (20 km) is above more than 90% of the earth's atmosphere. Application of MISR cloud-screening, cloud height retrieval, and cirrus detection algorithms require high-altitude operation. The normal

Manuscript received October 31, 1997; revised February 23, 1998. This work was supported by the Jet Propulsion Laboratory, California Institute of Technology, under contract with the National Aeronautics and Space Administration.

The authors are with the Jet Propulsion Laboratory, California Institute of Technology, Pasadena, CA 91109 USA (djd@jord.jpl.nasa.gov).

Publisher Item Identifier S 0196-2892(98)04162-X.

variation in aircraft roll, pitch, and yaw on the ER-2 as well as changes in altitude, track direction, and velocity, although small, must be measured. This information is required to georectify and coregister the image data for all angles and spectral channels. For MISR, we require that imagery from the nadir camera, projected to the surface terrain, be geolocated to ±275 m in both the cross-track and along-track directions and imagery of any particular target from the nine cameras be spatially coregistered with an uncertainty of ±275-m cross track and ±550-m along track, with a goal of ±275 m (all specifications are $2\sigma$). At minimum, AirMISR data must meet these requirements as well. However, because the spatial resolution of AirMISR data is much higher than MISR, we have established a goal for AirMISR of exceeding these requirements by a factor of ten.

## III. AirMISR Sensor Description

### A. General System Description

AirMISR is a pushbroom imager utilizing a single camera in a pivoting gimbal mount. A data run is divided into nine segments, each at a specific MISR look angle. The gimbal pivots aft between segments to repeat the pushbroom data acquisition of the same area on the ground from the next angle. This process is repeated until all nine look angles of the target area are collected. The swath width is governed by the camera field-of-view and varies from 11 km in the nadir to 32 km at the most oblique angle. The along-track image length at each angle is dictated by the timing required to obtain overlap imagery at all angles and varies from about 9 km in the nadir to 26 km at the most oblique angle. Thus, the nadir image dictates the area of overlap that is imaged from all nine look angles. The use of a single camera to provide coverage at all nine angles is made possible since we are not attempting to obtain continuous, global coverage, as is the case from EOS. Additionally, this approach ensures identical calibration at all angles, a useful feature in utilizing the instrument as part of the spaceborne MISR calibration.

The Jet Propulsion Laboratory (JPL), California Institute of Technology, Pasadena, adopted the following approach in developing the AirMISR instrument.

1) MISR brassboard, protoflight spares, and existing ground support equipment were adapted for the camera optics, electronics, and data system. This ensures that AirMISR is closely matched in spectral and radiometric performance to the spaceborne MISR. The use of existing components, assemblies, and facilities minimized the development costs.
2) The gimbal provides images at all nine MISR angles during a 13-min flight line. The computer-controlled gimbal supports a number of different operating modes, including the standard nine-angle sequence as well as alternative angle sequences for specific studies and algorithm validations.
3) MISR-equivalent pixels can be constructed by binning raw pixels in the ground data processing, taking into account the full resolution and frequency updates of existing Inertial Navigation System (INS) and Global Positioning System (GPS) pointing corrections as well as other look-angle scaling factors. From ER-2 altitude, the AirMISR camera has an instantaneous footprint of 7-m cross track × 6-m along track in the nadir view and 21 × 55 m at the most oblique angle. Lines of image data are acquired every 40.8 ms, resulting in an along-track sample spacing, regardless of view angle, of 8 m for an aircraft ground speed of 200 m/s. Thus, it is possible to generate samples that match MISR pixel dimensions at any view angle and compensate for the variable footprint dimensions with angle in the ground data processing. It is also possible to make use of the higher resolution imagery, if desired.
4) Sets of MISR calibration photodiode assemblies were incorporated into the design to test their ability to supplement laboratory calibrations. A detector-based calibration approach is one of the innovations included in the spaceborne MISR onboard calibrator and is essential to meeting the demanding radiometric accuracy requirements of the experiment. High-accuracy radiometry of AirMISR is necessary for it to provide a useful calibration pathway for the spaceborne instrument, and detector-based methods are also integral to AirMISR laboratory calibrations.
5) Room for an additional camera to be incorporated at a later date (e.g., to incorporate new spectral channels, or to enable the benchmarking of new technology camera components) was reserved within the instrument.

### B. Camera

The AirMISR camera consists of a MISR brassboard lens assembly mated to a spare camera head assembly. Both the lens and camera head meet all MISR performance requirements. The brassboard lens is a superachromatic, seven-element, refractive, f/5.5, telecentric design, rendered polarization insensitive to <1% uncertainty by a double-plate Lyot depolarizer. The full swath field-of-view is 30°. The brassboard was used by the MISR project to investigate packaging and mounting issues and was subsequently made available for use in AirMISR. The camera head is a fully assembled MISR engineering model spare and includes a four-element spectral filter, CCD focal plane array, stray light masks, and a passive thermal defocus compensation system that corrects for changes in focus due to temperature-induced variations in the lens refractive indices. The CCD architecture consists of four line arrays with 1504 active 21 × 18-$\mu$m pixels per line. The camera has its own camera head electronics (CHE) mounted to the camera head. Integration time is individually commandable for each of the line arrays up to a maximum value of 40.8 ms (the fixed line repeat time), and specific values are chosen for each band such that signal-to-noise ratio (SNR) specifications are met at the field edges, where transmittance is smallest. This causes the detectors to saturate at equivalent reflectances ranging from about 1.1 at field center to a value between 1.3 and 1.7, depending on band, at the field edges [3]. In a given band, equivalent reflectance $\rho$ is related to radiance $L$ via the relation $\rho = \pi L/E_0$, where $E_0$ is the band-weighted exoatmospheric solar irradiance.

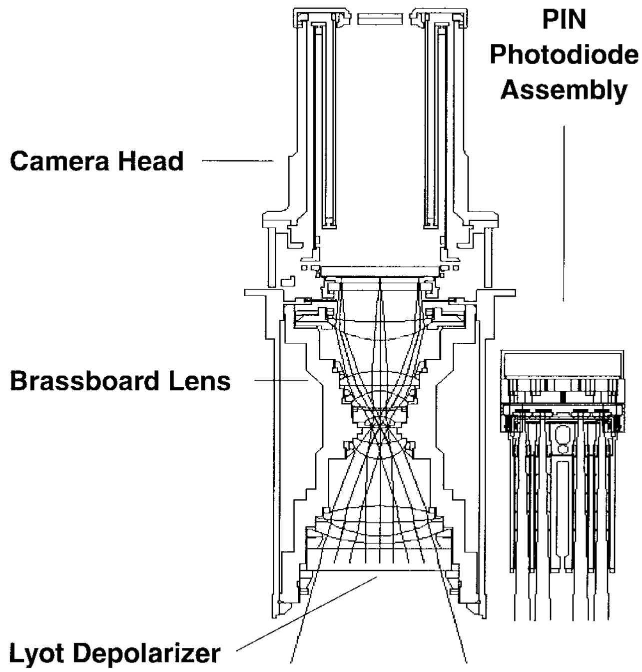


Fig. 1. Cross-sectional view of the AirMISR camera and PIN diode assembly.

An aluminum tube with mounting flanges was designed and fabricated to interface the lens to the camera head to form a full camera. The lens was centered on precision bores within the cylindrical part and held in place with a retaining ring. A stray light baffle that protects the detector from reflections was mounted to the cylindrical part with a retaining ring. The existing camera head mounting pads interface with the cylindrical part with shims to adjust focus and tilt between the lens and the detector. A flange on the outside of the cylindrical part bolts to an optical bench driven by the gimbal assembly. A cross-sectional schematic of the camera is shown in Fig. 1.

A laboratory calibration of the AirMISR camera was conducted and followed the same procedure used for the preflight calibration of MISR cameras. Detailed descriptions of the MISR preflight calibration procedures are provided by Bruegge *et al.* [6]. Two thermal vacuum chambers were used: the Optical Characterization Chamber (OCC) provides measurements of modulation transfer function (MTF), point spread function (PSF), effective focal length, optical boresight relative to the CCD array, and optical distortion; the Radiometric Calibration Chamber (RCC), along with an external 65″ integrating sphere and a monochromator provides SNR, light transfer response, and spectral characterization data. The sphere output was monitored with high-quantum efficiency (HQE) detector standards to provide a detector-based absolute calibration.

The camera effective focal length was determined to be 58.8 mm. MTF at 20 °C, the control set-point for flight, was measured at five field positions (±14.7°, ±10.3°, and 0°), and found to meet the required value of 0.24 at 23.8 cycles/mm with ample margin. The SNR was measured to be $\sim$190 at an equivalent reflectance of 0.02 and $>$700 at an equivalent reflectance of 1.0, thus, exceeding preestablished requirements. Due to a procedural error, suboptimal integration times for

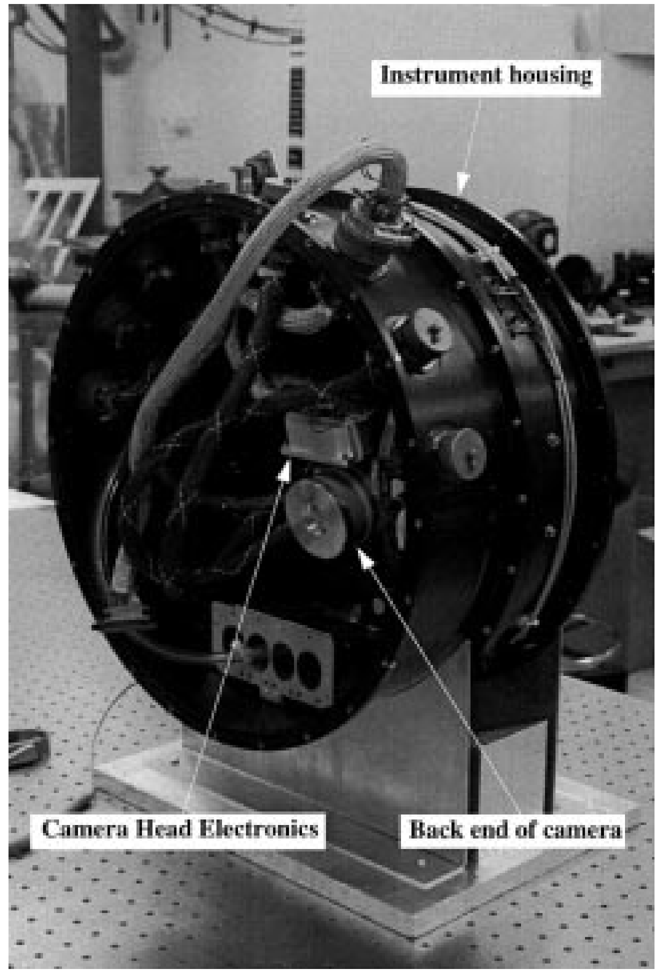


Fig. 2. Close-up view of AirMISR with the rear cover off, revealing internal cabling and the back of the camera. The cylindrical instrument housing is about 18″ in diameter.

assessing radiometric accuracy were used. This resulted in an estimated absolute radiometric uncertainty of 6% at full signal, instead of the required 3%. This was deemed adequate during the engineering checkout phase, but recalibration will be required for science operations. Plans call for recalibrating the camera at approximately semiannual intervals.

### C. Gimbal Assembly

The gimbal is driven by an Aerotech off-the-shelf actuator and controlled through an RS-232 interface. The rotary stage slews at about 20°/s and is accurate to 0.1°. The quick slewing helps to maximize the available ground swath length. Computer control of the gimbal allows for a variety of operational modes in addition to the standard nine look angles, including pitch offset correction, long flight lines at a single look angle, and a continuous scan mode useful for making test images, spatial calibration tests, and boresighting.

The camera gimbal assembly is covered by an aluminum cylinder and mounted between bearing blocks within a pressure housing. Fig. 2 is a photograph of the instrument, inside of which the back end of the camera can be seen. There is space on the gimbal assembly for a future, second camera. The housing containing the gimbal assembly is mounted in the ER-


Fig. 3. Rotating drum (which contains the camera) mounted on the bottom of the aircraft just ahead of the cockpit, before an engineering test flight in April 1997.

2 aircraft in an existing window frame (minus the window). When installed in the aircraft, the camera gimbal assembly axis is in a horizontal plane and is normal to the direction of flight. The camera gimbal-aluminum cylinder assembly protrudes beyond the lower surface of the aircraft fuselage.

Fig. 3 is a photograph of AirMISR mounted in the nose of the ER-2. A pressure box is built around the gimbal assembly to maintain 4-psi pressure inside the nose compartment. The sensor head experiences the outside ambient pressure, which drops to 0.7 psi at an altitude of 65 000 feet. The camera and rotary stage cabling is led out through a set of pressure bulkhead connectors to the instrument electronics rack above, and an O-ring seals the sensor head to the nose compartment skin. The gimbal assembly is rotatable to a stowed position, which points the camera directly forward, providing a light-tight sealed position inside the pressure box. This stowed position enables the collection of dark signal data during flight and protects the sensor optics during takeoff and landing.

### D. Detector-Based Calibration Photodiodes

A detector-based calibration approach is a unique feature of the EOS-AM1 MISR calibration system. This approach has been adopted in lieu of less-accurate source-based methods to meet the absolute radiometric accuracy requirements, including a 3% maximum uncertainty ($1\sigma$) at full signal. MISR uses both p-instrinsic-n doped (PIN) and HQE photodiodes with throughput defined by precision-built apertures to measure the radiance reflected from deployable Spectralon diffusers. PIN and HQE assemblies have been included in the AirMISR design to explore their utility as calibration standards, while viewing relatively uniform earth targets. A PIN photodiode assembly has been mounted to the rotating optical bench and boresight aligned to the camera (see Fig. 1). An engineering model filter/detector/electronics package was made available for use and a spare light baffle assembly was fabricated. A spare HQE assembly will be released from bonded stores for integration into AirMISR once EOS-AM1 has launched. Due to size constraints, the HQE assembly is fixed in the nadir-viewing direction. The camera and PIN photodiodes are aligned with the HQE fields-of-view when the gimbal is at the nadir-viewing position midway through a data run.

### E. Signal Chain and Data Handling

The instrument block diagram for the signal chain and data handling system is shown in Fig. 4. The analog signal from the cameras is digitized in the MISR engineering model camera support electronics (CSE) located just above the sensor head pressure box. The wiring on the CSE has been modified to accept inputs from the calibration photodiodes. Spare engineering telemetry channels in the CSE are used to digitize the signal from the PIN and HQE diode channels. All channels, including those carrying camera video, digitize a full 14 bits and include a precision voltage reference to calibrate the analog-to-digital-converters. The other engineering telemetry channels are used to monitor key diagnostic temperatures and voltages in the sensor head.

The remaining instrument electronics are mounted in a Lockheed-built ER-2 nose rack. The digitized camera and PIN diode data from the CSE are converted from serial streams to parallel words in the Camera-to-Computer Interface (CCI). The CCI can be expanded in the future to operate a two-camera configuration.

A Pentium-based workstation ruggedized for aircraft environments controls the instrument and the storage of digitized data. The computer receives “start data run” commands from a cockpit control panel. This initiates a preprogrammed data

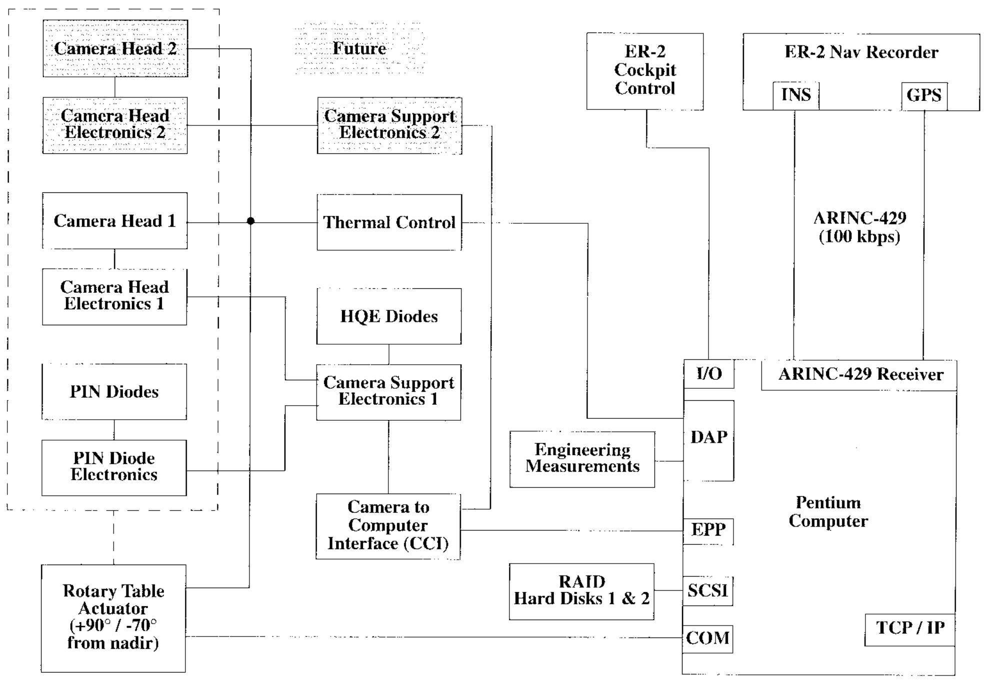


Fig. 4. AirMISR signal chain and data handling block diagram. Legend: ARINC = Aeronautical Radio, Inc.; COM = Communications; DAP = Data Acquisition Processor; EPP = Enhanced Parallel Port; GPS = Global Positioning System; INS = Inertial Navigation System; I/O = input/output; PIN = p-intrinsic-n; HQE = High Quantum Efficiency; RAID = Redundant Array of Inexpensive Disks; SCSI = Small Computer System Interface; and TCP/IP = Transfer Control Protocol/Internet Protocol.

acquisition and sensor pointing routine. At the end of the run, the camera is stowed out of the airstream at 90° from nadir (forward). The cockpit control panel also enables the pilot to abort the run and restart as required. The computer acquires the sensor data, photodiode data, and navigation data during the flight run and writes it to a ruggedized RAID level 1 hard disk system for downloading after the flight. The hard disks are contained within a hermetically sealed Ruggedtronics enclosure.

Aircraft INS and GPS navigation data are received at 100 kbps by a Condor CEI-200, two-channel ARINC-429 board in the onboard computer. Aircraft attitude is updated 64 times a second. Aircraft position (latitude and longitude) is updated eight times a second. Navigation data are recorded asynchronously, with respect to the camera data. The ARINC-429 time stamp included in both data sets is later used to align the navigation and camera time lines during processing.

### *F. Power Distribution and Ancillary Electronics*

The ER-2 supplies 115-V AC/400 Hz and 28-V DC power to the instrument. A Nova Electric Uninterrupted Power Supply (UPS)/Frequency Converter supplies the AC power to the 60-Hz loads through a central bus and provides keep-alive power to the computer while it performs an orderly shutdown when power is removed. A dedicated 28-V DC power supply is required to supply clean (±2% tolerance) power to the camera electronics. The aircraft 28-V DC supply is not adequately regulated for this task.

The thermal control system uses ER-2 28-V DC, which is pulsewidth modulated to control the power going to each of the thermal loops distributed around the instrument. Precision active temperature sensors and thermofoil heaters are used throughout, except for a platinum resistive temperature device (RTD) sensor in the hard disk. A single-board Microstar Laboratories data acquisition processor (DAP) located in the computer chassis controls the thermal loops, running independently of the main processor. Flexibility is designed to allow recovery from individual component failure without significant downtime and to allow compensation for thermal gradients if necessary.

## IV. Engineering Flights

For a new airborne sensor, engineering flights are typically held before the instrument can be considered operational for science missions. The objectives for AirMISR include testing the basic in-flight functionality, assessing the effects of aircraft pitch, roll, and yaw variations on image geometry, verifying the image radiometric quality, and ensuring that the instrument and aircraft work together in a flightworthy manner. Four engineering flights were held to attain flight qualification status.

### *A. Flight #1*

The first flight of AirMISR occurred on April 4, 1997. In order to protect the exposed optics from condensation that could result from inadvertent gimbal operation in flight at midaltitudes, i.e., takeoff to 40 000 feet, gimbal operation was programmed to interlock out in that range using inputs from altitude and landing gear switches. The ER-2 has an altitude switch that trips at 40 000 feet and a landing gear switch that activates when the gear is up. For this particular flight, the ER-2 was in the process of updating the altitude


Fig. 5. Red band raw data image at the 60° forward look angle from August 25, 1997.

switch and a simulated switch was implemented with pilot control. Preflight checkout could not verify operation of these switches because it is not possible in the hangar. Although the instrument collected ER-2 navigation data and engineering data in flight, it did not collect image data due to an anomaly in the simulated altitude switch. As a result of this experience, it was decided to remove the midaltitude interlock from the gimbal programming and rely on the pilot/operator to refrain from attempting data collection at midaltitudes.

### *B. Flight #2*

The second flight took place on April 11, 1997. Examination of the log files and engineering data files showed that power was cycled off by the pilot due to an instrument error indication (a light on the control panel) during the first two runs with attendant loss of thermal control for a sufficient duration (5–10 min) to cause the gimbal to become too cold for correct operation. As a result, the gimbal did not leave the stowed position. On the third run, thermal control was restored and the instrument collected a partial set of images, but they exhibited a high quantity of dropped lines and salt-and-pepper artifacts. These were not obvious in the most recent data taken on the ground. The dropped lines were determined to be due to insufficient write throughput at the RAID array, and the salt-and-pepper appearance was associated with background updates of the UNIX system clock, affecting the transfer of data from the CCI to the computer.

### *C. Flight #3*

Between the second and third engineering flights a number of instrument features were reworked. The most significant was replacement of the AIWA RAID array with dual 4-GB

(a)

Fig. 6. Color blue/green/red images acquired on August 25, 1997, at the (a) 26.1° forward look angle. Radiometric scaling using the preflight calibration coefficients and a simple line-by-line roll correction algorithm have been applied. The color bands have been spatially coregistered using tie pointing, and the data have been projected to a topographic map.

IBM drives functioning as a mirrored pair (RAID level 1). Software upgrades were also implemented. Laboratory testing showed this configuration to be significantly more robust, although rare line dropouts were still observed to occur. Since the frequency of dropped lines ($<0.1\%$) is low, and the ultimate uses of AirMISR data involve a degradation in spatial resolution from the raw imagery, this was not deemed to be a significant problem. Additionally, the criteria for indicating error messages (cockpit lights) were changed. The third flight took place on August 25, 1997. A complete set of images with very low line drops was collected on the first run shortly after reaching altitude. At the end of the first run during the return to stowed position, and during the second run, anomalous status messages from the gimbal controller were recorded in the log file. The pilot also noted that the cockpit run indicator light did not behave as expected. It is believed that this resulted from the gimbal controller electronics becoming too cold.

A reference target was chosen to be the middle of hangars to the northeast side of the Moffett Field runways. Center point coordinates are 37° 25.0′ N latitude and 122° 2.5′ W longitude. Overflight of the target while the instrument was viewing the nadir direction occurred at 2:12 p.m. PDT. Clear weather prevailed during the flight. The flight line azimuth was a heading of 190°, with respect to true north to duplicate orbital observing conditions of MISR. The solar zenith angle was 29.2°, and the solar azimuth angle was 205.8° at the time of overflight.

### *D. Flight #4*

During the third engineering flight in August, aircraft yaw tests had been conducted by the pilot to assess whether turbulent airflow beneath AirMISR affected the airstream at the aircraft pitot tubes, which are mounted on the fuselage behind AirMISR and provide airspeed readings. Flight safety considerations dictate that the measurements from both pitot tubes be in agreement, especially during approach and landing. The pilot simulated a crosswind landing by inducing 10° of yaw with the rudder during his landing approach. The airspeed indicator from the pitot tube “downwind” of the AirMISR drum became highly variable, with deviations up to 20 kts,

(b)

Fig. 6. (*Continued.*) Color blue/green/red images acquired on August 25, 1997, at the (b) 26.1° aftward look angle. Radiometric scaling using the preflight calibration coefficients and a simple line-by-line roll correction algorithm have been applied. The color bands have been spatially coregistered using tie pointing, and the data have been projected to a topographic map.

compared to the pitot tube in the clean airstream. Prior to the engineering flights, numerical aerodynamic simulations conducted by NASA Ames Research Center suggested that there would not be a significant influence of the instrument on the airspeed measurements. Based on the in-flight results, the fidelity of the theoretical simulations was improved and the effect was successfully modeled. Using these results, Ames recommended a structural extension of the pitot tubes by 10″. Lockheed agreed to this modification and completed the requisite design and fabrication. A test flight was conducted on November 4, 1997. Imagery was not obtained on this date due to a failure, just prior to flight, of a voltage regulator in the CSE. However, the pitot tube extensions improved the airspeed reliability as hoped, and AirMISR was declared to be flight qualified. The failed voltage regulator was subsequently replaced, and an additional flight was conducted on the next day, resulting in the collection of two full sets of images from orthogonal runs over Moffett Field. An aircraft-provided heater was successful in keeping the gimbal controller electronics warm and enabling proper operation.

## V. IMAGES

A subset of the data obtained on Flight #3 is used to illustrate the appearance of AirMISR imagery. The imaged area straddles the waters of San Francisco Bay near the inlet of Coyote Creek; mudflats and marshes; tidelands that are in part utilized as salt evaporation ponds; and urban areas of Mountain View, Sunnyvale, and adjacent communities that provide a grid of city streets, buildings, and an extensive network of freeways. These targets together provide a large array of surface reflectances as well as types of ground cover. The easily recognized geometric patterns of streets, runways, and shoreline will provide a basis for judging the accuracy of the data georectification results using the onboard navigation information.

The red band image at the forward-viewing 60° look angle is shown in Fig. 5. The only processing that was applied to the image was to flip it to compensate for image inversion by the camera lens and to orient it with north toward the top. Note that the raw data do not reflect the true along-track/cross-track

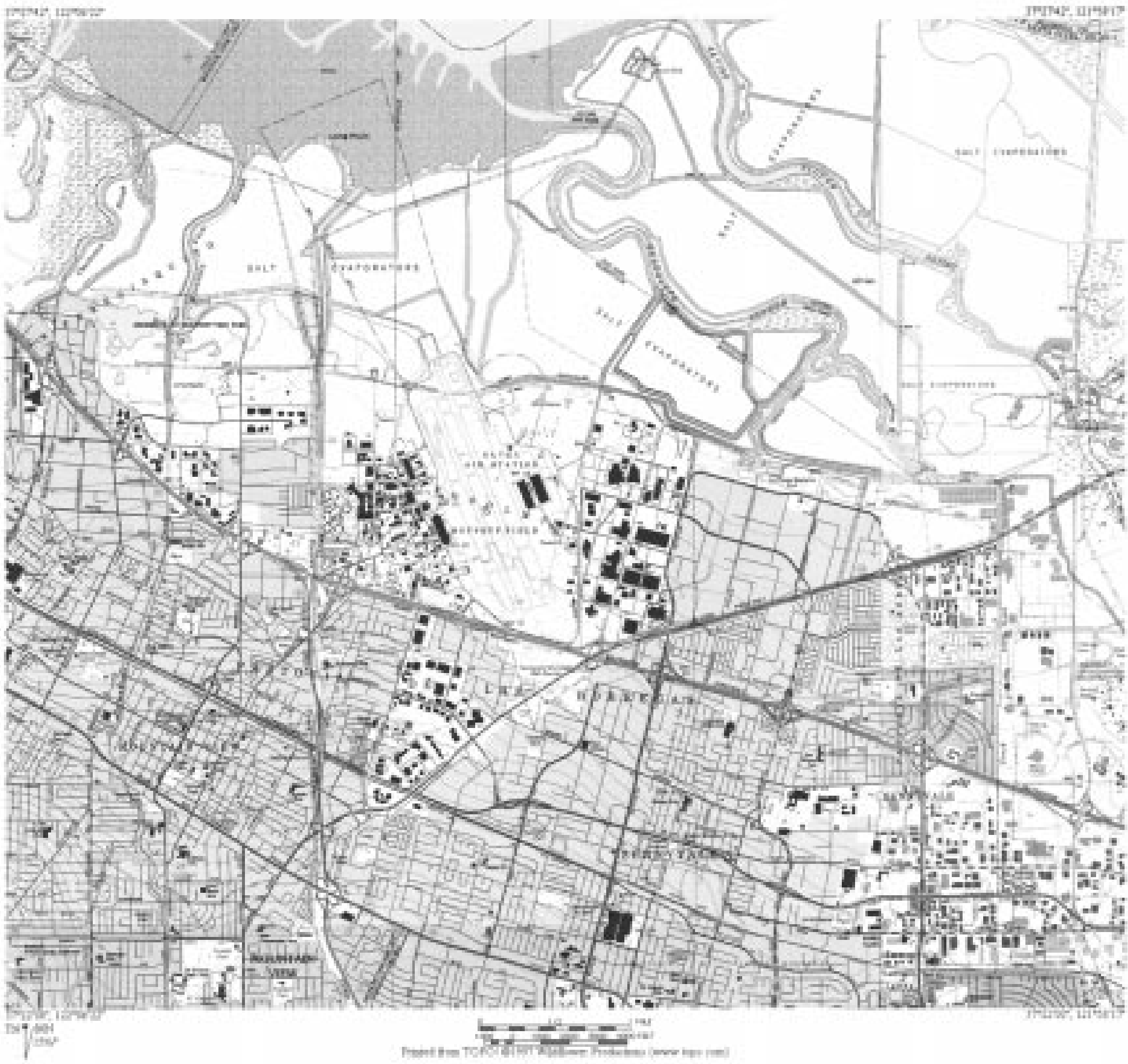

Fig. 7. United States Geological Survey topographic map of the area around Moffett Field. This map was printed from the TOPO! CD-ROM database, ©1997 Wildflower Productions.

spatial aspect ratio since at this view angle the cross-track sample spacing is 14 m and the along-track spacing is 8 m. When the data are resampled to a map projection, this will be corrected.

Several artifacts are apparent in the raw data. Near the top of the image are examples of the infrequent dropped lines. Below these is a segment of the image in which the pushbroom data appear "smeared" in the along-track direction. Comparison of AirMISR imagery with coincident ER-2 navigation data indicates that this type of feature occurs when the aircraft is pitching downward at a rate that compensates for the along-track motion, such that the same point on the ground is observed for multiple line times in each pixel. The required pitch rate for this "image motion compensation" to occur depends on look angle, with a smaller pitch rate threshold at the more oblique angles. For the 60° view angle, the required pitch rate is $-0.143°$/s.

A third artifact apparent in Fig. 5 is the "wiggly" appearance of linear features, such as the runways at Moffett Field near the bottom of the picture. This is due primarily to small variations in the aircraft roll angle. The high spatial resolution of the imagery, coupled with the high altitude of the aircraft, causes the typical roll angle variations of a few hundredths of a degree to be readily apparent in imagery of linear features. The high correlation observed between these artifacts and the aircraft navigation data imply that correction for attitude variations should be relatively straightforward.

As a first step in assessing the ability to correct for attitude variations, a simple roll correction algorithm was applied. This algorithm shifts each line of image data in the cross-track direction by the nearest integer number of pixels corresponding to the dynamic roll offset. This approach works best with nadir and near-nadir imagery due to the decoupling of roll from motion-induced artifacts from the other axes. More sophisticated attitude correction software that corrects for motions in all axes simultaneously requires a resampling of the imagery and is currently being tested and integrated into the AirMISR ground data processing flow. Preliminary indications are that this software is capable of removing significant attitude-induced artifacts from AirMISR imagery and the fidelity of ER-2 navigation data should be sufficient to meet our geolocation and coregistration goals. This is an important prerequisite to meeting our objective of distributing calibrated, geolocated, and coregistered data to the scientific community.

The results of the simple roll correction are shown in Fig. 6 for data at 26.1° view angle from the forward [Fig. 6(a)] and aftward [Fig. 6(b)] looks, respectively. These images have also been radiometrically scaled to account for pixel-to-pixel calibration differences and are composites of the blue-, green-, and red-band data. The bands were stretched individually to bring out the best contrast, which resulted in a slight modification of the true color; however, the same stretch was applied to both the forward and aftward data, thus, preserving the relative color balance between the two pictures. In generating these figures, the red band of the aftward image was map-registered to a 7.5′ topographic map using nearest-neighbor resampling within the ERDAS Imagine Geographic Information System (GIS) software package. The data in the nonred bands at the aftward angle and all bands of the forward angle were coregistered to the resampled aftward red band. The map registration accounts for the tilted boundaries of the images relative to the printed page since true north is at the top and the flight direction was not exactly due south. The wavy boundary on the right edge of each image shows the edge of the active pixel region and indicates the magnitude of the roll correction. The small residual nonlinearity of the runways is due to uncorrected variations in pitch and yaw. The high geometric fidelity of the corrected images is apparent from a comparison with the topographic map of the area around Moffett Field shown in Fig. 7.

With respect to image content, significant differences between the forward and aftward views in Fig. 6(a) and (b) are evident, particularly over water and tidal areas. Since the flight direction was southward (toward the sun), the forward view is observing light that has been forward scattered from the surface. A specular component of the reflection accounts for the greater brightness of such areas relative to the aftward view. Additionally, the aftward view has a somewhat "greener" appearance, which we speculate may be due to the proclivity of some vegetation toward enhanced backscatter. Other detailed differences between the forward and aftward views are apparent in many portions of the pictures.

## VI. Conclusions

Engineering flights of AirMISR have shaken out some initial "bugs," the instrument has been flight qualified, and high-quality sets of images and coincident navigation data have been successfully acquired. A few remaining issues need to be addressed. A mechanical clearance problem, which limited the camera's aftward rotation angle to 67.5° instead of the required 70.5°, will be corrected on the next flight. The MISR spare HQE diodes will be available for installation into AirMISR upon launch of the EOS-AM1 spacecraft; however, the absence of these diodes does not presently hamper science data collection, the ability to calibrate the camera in the laboratory, or radiometric scaling of the data. Finally, automated software to process AirMISR data radiometrically and use aircraft-supplied GPS and INS navigation data to geolocate and coregister the imagery, currently being tested, must be made operational.

For further information about MISR and AirMISR, the reader is invited to peruse our World Wide Web site at http://www-misr.jpl.nasa.gov.

## Acknowledgment

The authors gratefully acknowledge the assistance of D. Beckert, R. Deering, T. Fraschetti, B. Gaitley, M. Helmlinger, L. Hovland, D. Johnson, G. Saghri, C. Sepulveda, and P. Vera of the Jet Propulsion Laboratory and the helpful efforts of the NASA and Lockheed staff at Ames Research Center.

## References

[1] D. J. Diner, C. J. Bruegge, J. V. Martonchik, G. W. Bothwell, E. D. Danielson, V. G. Ford, L. E. Hovland, K. L. Jones, and M. L. White, "A Multi-angle Imaging SpectroRadiometer for terrestrial remote sensing from the Earth observing system," *Int. J. Imaging Syst. Technol.*, vol. 3, pp. 92–107, 1991.

[2] D. J. Diner, J. C. Beckert, T. H. Reilly, T. P. Ackerman, C. J. Bruegge, J. E. Conel, R. Davies, S. A. W. Gerstl, H. R. Gordon, R. A. Kahn, J. V. Martonchik, J.-P. Muller, R. B. Myneni, B. Pinty, P. J. Sellers, and M. M. Verstraete, "Multi-angle Imaging SpectroRadiometer (MISR) instrument description and experiment overview," this issue, pp. 1072–1087.

[3] C. J. Bruegge, V. G. Duval, N. L. Chrien, R. P. Korechoff, B. J. Gaitley, and E. B. Hochberg, "MISR prelaunch instrument calibration and characterization results," this issue, pp. 1186–1198.

[4] J. R. Irons, K. J. Ranson, D. L. Williams, R. R. Irish, and F. G. Huegel, "An off-nadir imaging spectroradiometer for terrestrial ecosystem studies," *IEEE Trans. Geosci. Remote Sensing,* vol. 29, pp. 66–74, Jan. 1991.

[5] J. V. Martonchik, "Determination of aerosol optical depth and land surface directional reflectances using multiangle imagery," *J. Geophys. Res.*, vol. 102, pp. 17 015–17 022, 1997.

[6] C. J. Bruegge, N. L. Chrien, B. J. Gaitley, and R. P. Korechoff, "Preflight performance testing of the Multi-Angle Imaging SpectroRadiometer cameras," in *Proc. SPIE 2957, Satellite Remote Sensing III,* Taormina, Italy, Sept. 23–26, 1996.

**David J. Diner**, for a photograph and biography, see this issue, p. 1040.

**Lisa M. Barge** received the B.S degree in geology from Oklahoma State University, Stillwater, in 1984.

She has been in the Science Data Processing Systems Section, Jet Propulsion Laboratory, California Institute of Technology, Pasadena, since 1984. She has been involved with numerous image processing projects in earth remote sensing and is currently involved with the Airborne Visible/Infrared Imaging Spectrometer (AVIRIS) and Multi-angle Imaging SpectroRadiometer (MISR) projects.

**Carol J. Bruegge**, for a photograph and biography, see this issue, p. 1086.

**Thomas G. Chrien** received the B.S. and M.S. degrees in optics from the University of Rochester, Rochester, NY, in 1984 and 1985, respectively, and the MBA from Pepperdine University, Malibu, CA, in 1991. He is currently pursuing the Ph.D. degree from the Rand Graduate School of Policy Studies, Santa Monica, CA, involving commercial and military applications of hyperspectral technology.

He has been with the Jet Propulsion Laboratory, California Institute of Technology, Pasadena, since 1985 and is currently a Senior Optical Engineer in the Imaging and Spectrometry Systems Technology Section, investigating applications of imaging spectroscopy. He has taught several courses on hyperspectral imaging and the calibration of imaging spectrometers.

**James E. Conel**, for a photograph and biography, see this issue, p. 1086.

**Michael L. Eastwood** received the B.S. degree in engineering from the University of California at Irvine in 1982.

He has been with the Jet Propulsion Laboratory, California Institute of Technology, Pasadena, since 1989 and is currently Leader of the Airborne Visible/Infrared Imaging Spectrometer (AVIRIS) engineering team. He has been responsible for several performance-enhancing modifications to the AVIRIS instrument, including focal plane arrays and optical system refinements. His experience with the Ames ER-2 flight operations personnel and facilities drew him into the job of facilitating the introduction of AirMISR into ER-2 flight operations.

**Jose D. Garcia** received the B.S. degree in electronic engineering from California State University, Los Angeles, in 1991.

He has been with the Jet Propulsion Laboratory, California Institute of Technology, Pasadena, since 1985. Since joining JPL, he has been involved with CCD detectors camera systems development. He has worked on several NASA flight projects, including Wide-Field/Planetary Camera 2 (WFPC-2), Solar X-Ray Telescope (SXT), Mars Rover Rear-Color Camera, and Multi-angle Imaging SpectroRadiometer (MISR), and currently provides instrument engineering support to AirMISR.

**Marco A. Hernandez** received the A.A. degree from Pasadena City College, Pasadena, CA, in 1988.

He served in the United States Air Force as an Airframe Structural Repair Specialist. He has been with the Jet Propulsion Laboratory, California Institute of Technology, Pasadena, since 1984, supporting various projects, including Wide-Field/Planetary Camera for the Hubble Space Telescope, the Near Infrared Mapping Spectrometer (NIMS) on the Galileo Orbiter, and the Airborne Visible/Infrared Imaging Spectrometer (AVIRIS). Presently, he is an Engineering Member of the Technical Staff, assigned to AirMISR.

**Charles G. Kurzweil** received the B.S. degree in mechanical engineering from California State University, Los Angeles, in 1974.

He has been with the Jet Propulsion Laboratory, California Institute of Technology, Pasadena, since 1957 and has been involved with many NASA planetary and earth remote-sensing instruments, including the Airborne Visible/Infrared Imaging Spectrometer (AVIRIS) and the Airborne Emissions Spectrometer (AES). He is currently the Mechanical Designer of AirMISR.

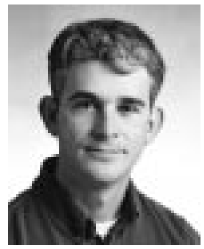

**William C. Ledeboer** received the B.S. degree in engineering and applied science with honors from the California Institute of Technology, Pasadena, in 1981 and the M.S. degree in computer science from the University of Southern California, Los Angeles, in 1994.

He has been with the Jet Propulsion Laboratory, California Institute of Technology, since 1985 and is currently a Member of the Multi-angle Imaging Science Element in the Earth and Space Sciences Division. He has worked on numerous NASA planetary missions and is presently the Science Data Validation Software Engineer for the EOS Multi-angle Imaging SpectroRadiometer (MISR) experiment and its airborne counterpart, AirMISR.

**Neil D. Pignatano** received the B.S. degree in physics from the State University of New York at Stony Brook in 1977.

He has been with the Jet Propulsion Laboratory, California Institute of Technology, Pasadena, since 1979 and has been involved in many NASA planetary and astronomical projects. He is currently the Technical Group Supervisor of the Multi-angle Imaging SpectroRadiometer (MISR) Electronics, Detectors, and Ground Support Equipment Group, Observational Systems Division, as well as the Project Element Manager for AirMISR.

**Charles M. Sarture** received the B.S. degree in electronic engineering from the University of Southern California, Los Angeles, in 1981.

He has been with the Jet Propulsion Laboratory, California Institute of Technology, Pasadena, since 1981 and is currently Instrument Manager and Instrument Engineer of the Airborne Visible/Infrared Imaging Spectrometer (AVIRIS), which he has been involved with since 1989. He has worked on AirMISR from concept and continues to provide instrument engineering support. He has also been involved in development and test of the Galileo spacecraft Attitude and Articulation Control Subsystem.

**Bruce G. Smith** received the B.S. degree in computer science with honors from the University of California, Santa Cruz, in 1982.

He has been with the Jet Propulsion Laboratory, California Institute of Technology, Pasadena, since 1993. He has provided software support for the Multi-angle Imaging SpectroRadiometer (MISR) Ground Support Equipment, and since joining the AirMISR team, he has been responsible for the design and development of the instrument flight software.